Available online at www.sciencedirect.com
ScienceDirect
Applied Catalysis B: Environmental 78 (2008) 166–175
APPLIED CATALYSIS B: ENVIRONMENTAL
www.elsevier.com/locate/apcatb

Washcoating of Pt-ZSM5 onto aluminium foams

Oihane Sanz [a], Luciano C. Almeida [a], Juan M. Zamaro [b], María A. Ulla [b], Eduardo E. Miró [b], Mario Montes [a,*]

[a] *Grupo de Ingeniería Química, Facultad de Químicas, UPV/EHU, Apdo. 1072, 20080 San Sebastián, Spain*
[b] *INCAPE (Instituto de Investigaciones en Catálisis y Petroquímica) FIQ-UNL, CONICET, Santiago del Estero 2654, 3000 Santa Fe, Argentina*

Received 20 June 2007; received in revised form 13 September 2007; accepted 15 September 2007
Available online 21 September 2007

Abstract

The anodisation conditions of aluminium foam monoliths are studied in order to produce alumina with controlled properties. When anodisation conditions are extreme, an important cracking of the surface appears with width and depth cracks that depend on the anodisation parameters, i.e., electrolyte temperature, anodisation time and applied current density. Different surface treatments for aluminium foams (rough anodisation, smooth anodisation, and no anodisation) were used to observe the mechanical stability of Pt/ZSM5 coatings. Roughness of the surface improved adhesion of Pt/ZSM5 coatings because the size of the cracks was high enough to occlude the zeolite particles promoting a mechanical anchorage of the coating. The washcoated aluminium foam monoliths were tested in total oxidation of toluene showing very high activity.

Keywords: Aluminium foams; Anodisation; Zeolite washcoating; Catalyst coating adhesion

1. Introduction

Monolithic catalysts have become one of the most relevant and economically significant application of catalytic reactor engineering and industrial catalysis so far. This is due to the commercial success of such well-known environmental catalysis processes, as the purification of exhaust gases from automobiles, the abatement of NOx emitted in the stack gases from power stations by selective catalytic reduction processes, and the catalytic combustion of VOCs. In recent years foam monoliths have been applied in the catalysis field as supports because of the advantages resulting from their structure [1,2]. Monoliths with longitudinal parallel channels usually develop laminar flows, whereas foams have extensive pore tortuosity that produces turbulent flow, improving mixing and transport phenomena [3–5].

The most common material for monolithic structures is cordierite because this material is very well suited for the requirements of automotive industry [6]. The main reasons are their high mechanical strength, their resistance to high temperatures and temperature shocks, and their low thermal expansion coefficient [7].

However, under certain circumstances, it is preferable to use metallic substrates since they present a series of comparative advantages with respect to ceramics, i.e., higher mechanical resistance, higher thermal conductivity, and better prospects of achieving high cell densities [8]. Nevertheless, the preparation of metallic monoliths has a critical point, i.e., the adhesion of the catalytic coating to the metallic substrate. When coating metallic supports with a catalytic material, an intermediate layer of ceramic material is often used for better binding. Many different metals and alloys have been proposed for the manufacturing of metallic monoliths in the search for mechanical, chemical and thermal stability and availability in thin foils. In addition to some Ni and Cr alloys, steel is the most widely used alloy, especially ferritic alloys containing Al that can produce alumina scales improving the adhesion deposited on it [9]. When the working temperature is not so high as in automotive exhausts, another interesting material to prepare metallic monolith is aluminium. It has excellent mechanical and thermal properties to be used as structural material [10,11]. Moreover, aluminium can be coated with alumina obtained anodisation and their texture can be controlled by tuning up the anodisation parameters. Burgos

* Corresponding author.
E-mail address: mario.montes@ehu.es (M. Montes).

0926-3373/$ – see front matter © 2007 Elsevier B.V. All rights reserved.
doi:10.1016/j.apcatb.2007.09.024

et al. [12] published an extensive study on aluminium sheet anodisation to prepare metallic monoliths. They analyzed the influence of anodisation time, current density, electrolyte nature, its temperature and concentration, and the effect of agitation on the final alumina textural properties. The alumina generated by anodisation with H_2SO_4 is amorphous and remains amorphous until 800 °C, when the γ-Al_2O_3 phase is detected [12].

A monolithic structure can be coated with a catalytic support layer to increase the specific surface area and hence to improve and stabilise the dispersion of the active phase [6]. This coating is usually obtained by washcoating. The monolith is dipped in a slurry prepared with the catalytic material and after a certain time, withdrawn carefully. The characteristics of the final coating are a complex function of monolith properties, slurry properties and preparation conditions [13]. It has been shown from results of different laboratories that the adhesion of the coating depends primarily on the particle size of the deposited powders. Agrafiotis et al. [14–16] studied the effect of powder characteristics and processing parameters on the properties of alumina, zirconia and titania washcoats deposited on ceramic supports. They concluded that adhesion of the washcoat layer on the support takes place primarily by a mechanical mechanism and to a much lower extent via chemical or affinity mechanisms. Zamaro et al. [17] reported results of ZSM5, mordenite and ferrerite washcoated on a cordierite monolith. They observed that the stability order correlates well with the size of zeolite aggregates: higher adhesion is obtained with lower sizes. Bigger aggregates cannot enter inside the cordierite pores; thus poor adhesion is obtained. Cini et al. [18] reached similar conclusions. They observed that to enhance the mechanical adhesion of the coated layer, the size of the washcoat particles must be smaller than the size of the support macropores.

This work is focused on the preparation and characterization of anodic aluminium oxide layers onto aluminium foam monoliths for Pt-ZSM5 washcoating. The main objective of this study is to find good anodisation conditions for aluminium foam monolith to obtain a mechanically stable washcoating with catalytic activity for VOCs abatement. The anodisation variables studied are electrolyte temperature, anodisation time and applied current density.

2. Experimental

2.1. Preparation of structured supports

The 10 ppi aluminium foams (Alloy AA6101) used in this work (see Fig. 1) were manufactured by ERG Materials and Aerospace (DUOCEL) and their composition is shown in Table 1. Monoliths were cut out from slabs (40 mm of width) using a hollow drill with a diamond saw of 16 mm of internal diameter. After cutting, they were washed with water and acetone and finally dried.

Table 1
Weight percentage of the composition of the aluminium foam (alloy AA 6101)

Metal	Mg	Si	Fe	Cu	Zn	B	Cr	Mn	Al
%	0.6	0.5	0.5	0.1	0.1	0.06	0.03	0.03	98

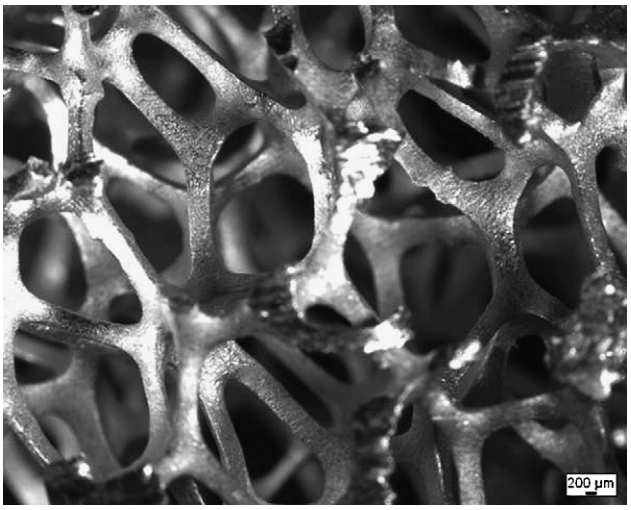

Fig. 1. General view of the original aluminium foam.

Anodisation was carried out in an anodisation polypropylene tank with 2.55 M sulphuric acid. Temperature control of +/−0.1 °C was obtained with a cooling PTFE coil connected to an external chiller, and an electrical heater by a PID temperature controller. The Agilent HP 6692 A Power Supply used can operate between 0–60 V and 0–110 A allowing current or voltage control. All the experiments were carried out at constant current density, and the voltage showed the classical variation with a sharp peak at the beginning of the process which decreases slowly until a constant value was reached [12]. The aluminium monolith was fixed to the anode (working anode) with titanium brackets and this assemble was placed between two aluminium foils connected to the cathode (counter-electrodes). A vigorous air bubbling assured the agitation inside the bath. Only 30 mm of the 40 mm of the monoliths were immersed into the electrolyte, leaving the titanium brackets outside the electrolyte in order to assure the electrical continuity during the anodisation process. After anodising, monoliths were taken out of the electrolytic bath, thoroughly washed with water to take out the acid, and they were dried at 60 °C during 1 h and calcined at 600 °C for 2 h. Finally, 25 mm of the bottom part which was homogeneously anodised were cut and used.

The effect of the anodisation conditions on the textural properties of the alumina electro-generated on the monolith was studied. Bath temperature was varied between 10 and 60 °C, anodisation time between 5 and 40 min, and current density was changed in the range of 2–6 A per monolith.

2.2. Powder catalyst preparation

NH_4-ZSM5 zeolite (Zeolyst CBV 3024, Si/Al = 15) was used to prepare the catalyst. The 1% Pt-ZSM5 catalyst was prepared via incipient wetness impregnation with $Pt(NH_3)_4(OH)_2$ aqueous solution. Concentration was calculated in order to introduce 1% Pt into the pore volume. After the

impregnation, the platinum catalyst was dried for 1 h in an oven at 120 °C and calcined at 600 °C for 6 h.

2.3. Washcoating

Based on previous results [17] an aqueous slurry of the catalyst with a 15 wt.% solids content of slurry of the catalyst was used for washcoating the foam monoliths. The foam monoliths were coated as follows: they were dipped in the slurry at 3 cm/min and maintained immersed for 1 min. They were pulled out at the same speed and the excess of the slurry was eliminated by centrifugation at 400 rpm for 10 min. Afterwards, they were dried at 120 °C for 2 h and weighted. This washcoating procedure was repeated one or two times successively and finally the monoliths were calcined at 600 °C for 2 h.

2.4. Catalytic activity

The catalytic activity of the washcoated foam monoliths was tested in the complete oxidation of toluene in air. Total flow rate used was 1000 cm^3/min (GHSV = 12000 h^{-1}) and toluene concentration was 1000 mg C/m^3. The catalyst was pretreated in air at 400 °C for 1 h prior to the reaction and the ignition curves were obtained under a heating ramp (100–400 °C at 2.5 °C/min). Conversion was calculated by measuring toluene disappearance and the production of water by Mass Spectroscopy (Balzers Omnistar), together with CO_2 measurement by an on-line IR detector (Sensotrans IR). The agreement observed for all the samples between the three conversion curves obtained using signals of toluene, water and CO_2 confirmed the very high selectivity for complete oxidation without formation of significant amounts of intermediate products.

2.5. Characterization

Particle size distributions of the NH_4-ZSM5 zeolite and 1% Pt-ZSM5 catalyst powders were measured with the aid of a laser particle size analyzer (MasterSizer 2000 of MALVERN). 100 mg of solid were dispersed in 10 ml H_2O in a ultrasound bath for 1 h before the measurement. The Zeta Potential was measured by using a MALVERN Zetasizer 2000 instrument. The particles of the solids were dispersed in an aqueous solution of 0.003 M NaCl. pH was adjusted with HNO_3 or NaOH solutions for both solids. Adhesion of the coatings was evaluated in terms of weight loss after ultrasonic treatment [19]. The calcined coated foams were immersed in petroleum ether inside a sealed beaker, and then treated in an ultrasound bath for 30 min. The weight loss was calculated by difference and referred to as percentage of the amount of coating.

Textural properties were studied by N_2 adsorption (Micromeritics ASAP 2020) using a home-made cell which holds the entire 5 cm^3 foam monoliths. BET surface area (accuracy better than 10% for low area samples and better than 2% for the rest of the samples), total pore volume and pore size distribution are obtained. The amount of alumina generated during anodisation was determined by gravimetry (accuracy better than 3%). It was calculated from the weight difference between the anodised aluminium foam before and after a chemical treatment that dissolves selectively the alumina. The dissolving solution contained 35 ml of phosphoric acid (PROBUS 85%) and 20 g of chromic acid (PANREAC) dissolved in distilled water to 1 l. The dissolution process was carried out at 80–100 °C for 10 min [20]. Conventional SEM micrographs were taken from several samples (HITACHI S-2700). The samples were previously gold sputtered for 2–2.5 min in a SC 500 SPUTTER COATER.

3. Results

Table 2 presents the influence of the anodisation conditions, i.e., time, temperature and current density on the amount and properties of the anodisation coating. The amount of alumina generated per monolith (g Al_2O_3/monolith) was calculated from the oxide dissolution with the phosphoric–chromic acid solution. The total surface area of each foam monolith

Table 2
Properties of the anodisation layer for different anodisation conditions with 2.55 M sulphuric acid

t (min)	T (°C)	Current density (A/monolith)	g Al_2O_3/monolith	$S_{monolith}$ (m^2/monolith)	S_{BET} (m^2/g Al_2O_3)	$V_{p\text{-}monolith}$ (cm^3/monolith)	V_p (cm^3/g Al_2O_3)	D_p (nm)	Thickness (μm)
20	**10**	2	0.2028	2.84	14.0	0.010	0.049	9	20
20	**20**	2	0.2106	3.23	15.3	0.013	0.062	9.5	20
20	**30**	2	0.2135	4.42	20.7	0.017	0.080	10.5	20
20	**40**	2	0.1227	5.77	47.0	0.030	0.244	17.5	20
20	**50**	2	0.0390	2.74	70.3	0.010	0.256	15	10
20	**60**	2	0.0105	1.27	121	0.004	0.381	12	5
5	30	2	0.1231	0.96	7.80	0.002	0.016	7	5
10	30	2	0.1370	1.98	14.5	0.010	0.073	8.5	10
20	30	2	0.2135	4.42	20.7	0.017	0.080	10.5	20
40	30	2	0.1744	8.71	49.9	0.056	0.321	20.5	45
20	30	**2**	0.2135	4.42	20.7	0.017	0.080	10.5	20
20	30	**4**	0.3572	7.08	19.8	0.032	0.090	16.5	70
20	30	**6**	0.5098	9.01	17.7	0.051	0.100	18	90
20	40	**2**	0.1227	5.77	47.0	0.030	0.244	17.5	20
20	40	**4**	0.3627	9.81	27.0	0.055	0.152	22	60
20	40	**6**	0.3987	10.9	27.3	0.067	0.168	25	80

Bold values shows the preparation variable changing in every of the four sub-series.

($S_{monolith}$, m^2/monolith) is directly obtained by applying the BET equation to the nitrogen adsorption data. The specific surface area of the alumina generated (S_{BET}, m^2/g Al_2O_3) was calculated by dividing the area measured by nitrogen adsorption for the anodised monoliths by the amount of alumina calculated from gravimetry. The pore volume generated in the alumina per monolith ($V_{p\text{-}monolith}$, cm^3/monolith) was given by the nitrogen adsorption measurement. The specific porosity of the alumina (V_p, cm^3/g Al_2O_3) was obtained by dividing the pore volume by the oxide amount of the monolith. The mean pore diameter (D_p, nm) was also given by the nitrogen adsorption measurement, assuming cylindrical pores. Finally, thickness (μm) refers to the alumina layer thickness, and it was an approximated value obtained from several SEM micrographs (±20%).

Experiments at different temperatures between 10 and 60 °C were carried out keeping the current density (2 A/monolith) and the anodisation time (20 min) constant. An increment in temperature from 10 to 40 °C produced an increase in the pore size and also in porosity of the oxide layer. However, the porosity increase was much more important suggesting an increase also in the number of pores produced. Nevertheless, the total pore volume, the amount of alumina, the total surface area and the thickness of the alumina layer decreased drastically when increasing temperature from 40 to 60 °C. In contrast, the generated alumina was four times more porous and the specific surface area of the alumina also increased. This effect shows that the increase of the oxide dissolution with temperature is more important than the increase of the oxide formation.

Textural properties of the alumina layer were also affected by the anodisation time (see Table 2). The amount of alumina per monolith and all the related parameters increased as the anodisation time increased from 5 to 20 min (30 °C and 2 A/monolith). However, for 40 min, the amount of alumina remaining on the aluminium surface decreased in spite of the increase in surface area, porosity and pore size. This result suggests that something new is being produced at long anodisation time that modifies the trend observed at shorter times.

The increase in current density from 2 to 6 A/monolith (20 min, 30 °C) produced an increase in the amount of alumina generated and, in consequence, a parallel increase in total surface area and porosity. Nevertheless, the specific surface area of the alumina decreased slightly and their porosity increased slightly. The size of the pores passed from 10.5 to 18 nm showing that the dissolution of the alumina inside the pores increased.

The same variation in current density at 40 °C produced similar results but with a higher decrease in specific surface area of the alumina and a decrease in their specific pore volume. The size of the pores was larger indicating that the re-dissolution of the alumina inside the pores increased with temperature.

Surface roughness has been studied by SEM (×3000 magnification). Fig. 2 shows the surface of the raw material (DUOCEL aluminium foam) as received from the manufacturer. The surface is uneven presenting hollows or bumps (just turn 180° the image) from 1 to 10 μm diameter and about

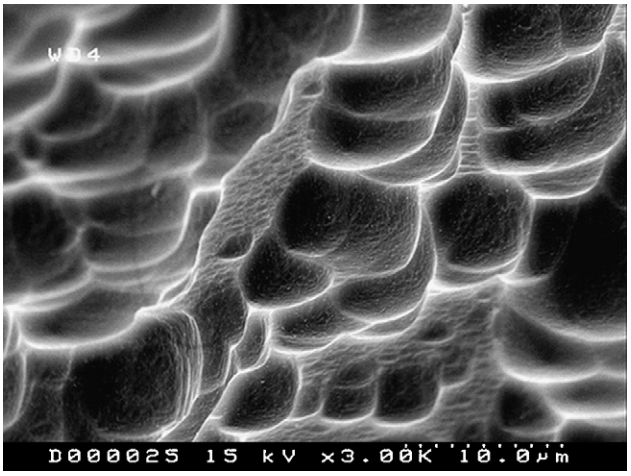

Fig. 2. Micrograph of aluminium foam surface.

0.5 μm depth. The same morphology has been reported by other authors for the same material [21]. Fig. 3 presents the influence of anodisation temperature of the series prepared for 20 min with 2 A per monolith. From 10 to 30 °C, the anodised surface reproduced the original roughness. However, at 40 °C a new relief appeared. The complete surface was covered by irregular slits with crests spaced out around 2 μm and around 2–4 μm depth (measured in several lateral views not shown). It is worth pointing out that the average thickness of the alumina layer is around 20 μm and therefore, this new morphology corresponds to no more than 10–20% of the layer being the rest conventional porous but compact alumina. The same surface morphology but at reduced scale is observed as temperature increases to 50 and 60 °C. A similar decrease was also detected in the total thickness of the alumina layer.

Fig. 4 shows the effect of anodisation time (at 30 °C and 2 A per monolith) on the surface roughness. Surface cracking is a phenomenon that appeared only after 40 min. Fig. 5 presents the influence of the current density (2, 4 and 6 A per monolith) at 30 °C (left column) and 40 °C (right column) on the surface roughness of the monoliths anodised for 20 min. At 30 °C the cracking phenomenon did not appear, but at 40 °C cracks appeared and grew in size as the current density increased.

Fig. 6 presents the Zeta Potential measurements of the NH_4-ZSM5 and the Pt/ZSM5 powders, showing both the isoelectric point at around pH 1. The particle size distribution of both powders is presented in Fig. 7. The main particle size for NH_4-ZSM5 was 4.5 μm and 90% of the powder was smaller than 8.5 μm. Pt/ZSM5 presented a main particle size of 3 μm and 90% was smaller than 6.25 μm.

Table 3 presents the main properties of the materials used to washcoat the monoliths: ZSM5, the Pt/ZSM5 catalyst and the aluminium monoliths. Three types of aluminium foam monoliths and two different anodisation conditions were used:

- 40 °C, 20 min and 6 A/monolith that produced a rough surface with cracks ($Monolith_{Rough}$);
- 30 °C, 20 min and 6 A/monolith that produces a smooth surface ($Monolith_{Smooth}$);
- non-anodised monoliths ($Monolith_{NA}$)

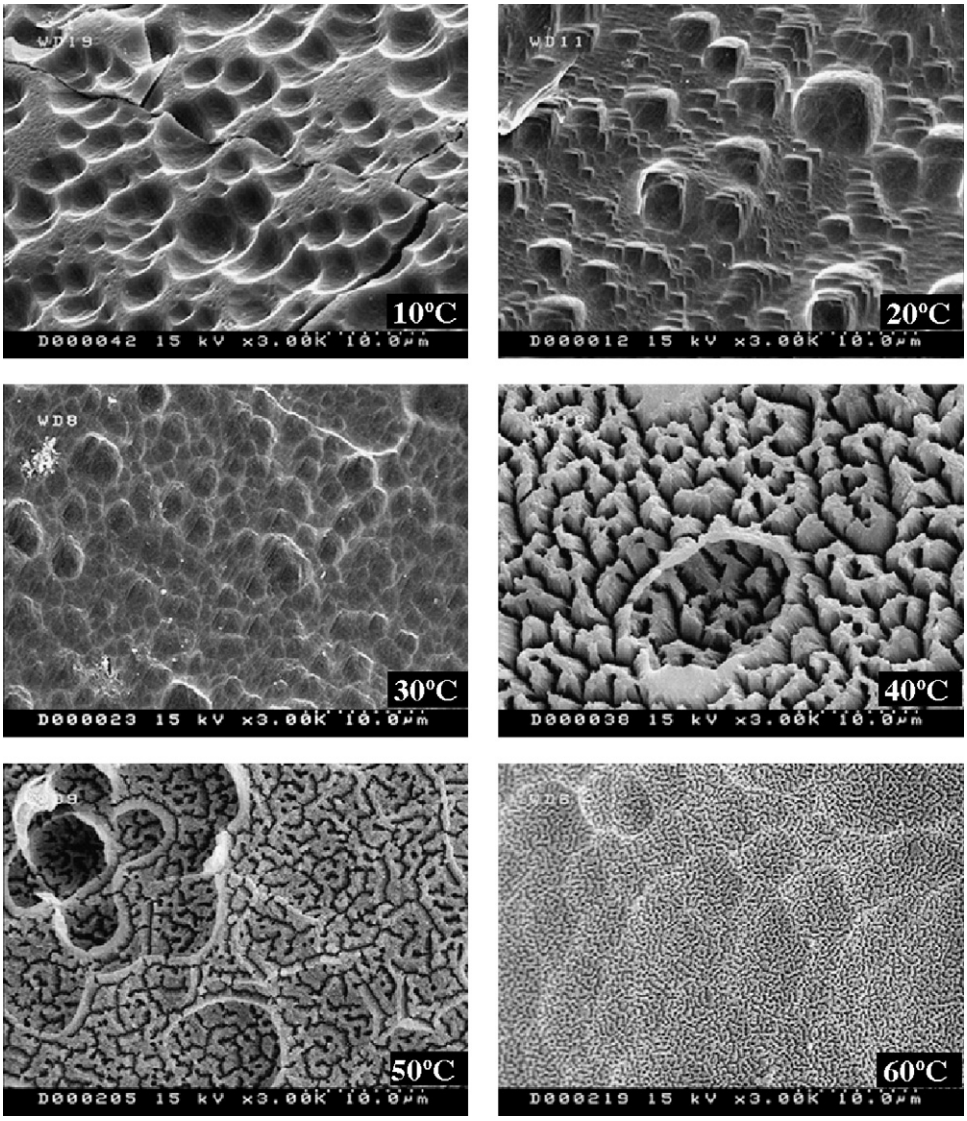

Fig. 3. SEM micrographs. Effect of anodisation temperature on alumina layer (2.55 M H_2SO_4, 20 min and 2 A/monolith).

To compare foams and honeycombs a longitudinal parallel channel monolith (350 cpi) of anodised aluminium [12] was also studied ($Monolith_{PC}$).

In this table, the structured catalysts prepared from these monoliths and powders are also presented. Notation used includes the monolith reference and 0, 1 or 2 W code to indicate the monolith as anodised (0 W), after one washcoating (1 W) and after two washcoatings (2 W). The sample referred to as $monolith_{Smooth}$/Pt correspond to a smooth anodised monolith without zeolite coating but with Pt impregnated on

Table 3
Properties of the washcoated monoliths and materials used

Name	g Pt-ZSM5	mg Pt/monolith	S_{BET} (m^2/monolith)	V_p (cm^3/monolith)	D_p (nm)	Thickness Pt-ZSM5 (μm)	% Weight loss
$Monolith_{Smooth}$ 0W	–	–	9.01	0.051	18	–	–
$Monolith_{Smooth}$ 1W	0.0106	0.11	14.7	0.054	16.5	6	85
$Monolith_{Smooth}$ 2W	0.0284	0.28	20.7	0.056	16	14	80
$Monolith_{Smooth}$/Pt	–	1.15	10.6	0.058	18.5	–	–
$Monolith_{Rough}$ 0W	–	–	10.9	0.067	25	–	–
$Monolith_{Rough}$ 1W	0.0179	0.18	19.4	0.072	27	7	48
$Monolith_{Rough}$ 2W	0.0328	0.33	23.8	0.075	27	11	40
$Monolith_{NA}$ 1W	0.0116	0.12	–	–	–	–	95
$Monolith_{NA}$ 2W	0.0215	0.21	–	–	–	–	90
$Monolith_{PC}$ 0W	–	–	19.5	0.068	14.6	–	–
$Monolith_{PC}$ 1W	0.0153	0.15	28.6	0.080	14.9	–	–

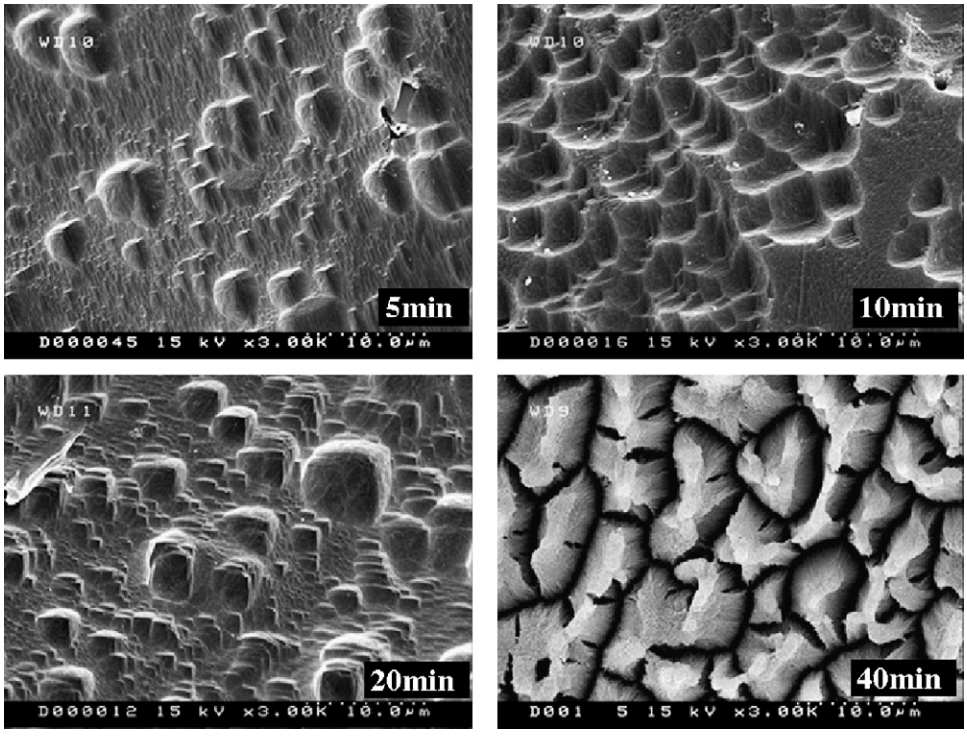

Fig. 4. SEM micrographs. Effect of anodisation time on alumina layer (2.55 M H_2SO_4, 30 °C and 2 A/monolith).

the porous alumina layer. The different columns present the amount of Pt-ZSM5 powder fixed by washcoating (g Pt-ZSM5), the amount of Pt (mg Pt/monolith), the total surface area of the washcoated monolith (S_{BET}, m^2/monolith), the total pore volume of the washcoated monolith (V_p, cm^3/monolith), the pore size (D_p, nm), the approximate coating thickness produced by the washcoating measured by SEM (thickness Pt-ZSM5, μm) and the weight loss after the adhesion test (% weight loss).

It can be seen that the amount of catalyst loaded by washcoating was higher on the rough foam monolith than in the smooth one and the non-anodised one. It can also be calculated that the increase in surface area and pore volume was proportional to the amount of Pt/ZSM5 and their corresponding textural properties (S_{BET} = 349 m^2/g and V_p = 0.25 cm^3/g). The second washcoating produced an additional load similar for both smooth and rough foam monoliths, and a slight lower load on the non-anodised one. Pore size distributions of the smooth and rough foam monoliths are presented in Fig. 8. A clear difference between the initial smooth and rough foam monoliths was observed. This difference was preserved after the washcoating procedure. The rough foam monoliths presented a wider distribution with a maximum at around 25 nm and the distributions of the smooth ones are narrower with the maximum at 18 nm.

The adhesion of the washcoating evaluated by the weight loss after the ultrasound treatment showed a clear difference as a function of the surface roughness. The smooth foam monoliths lost 80–85% of the catalyst loaded, and the rough ones only 40–48%. No anodised foam monoliths lost almost all the coating, 90–95%.

Lateral views of the rough and smooth foam monoliths before and after second washcoating are presented in Figs. 9 and 10, respectively. The lateral view of the rough foam monolith shows cracks with a depth of around 10 μm (Fig. 9). In the SEM lateral view of the alumina layer covered with zeolite (Fig. 10), it can be seen that the particles of the zeolite are inserted in the cracks of the rough monolith (Rough 2 W). On the other side, in the smooth monolith (Fig. 10, Smooth 2 W) the physical interaction between the zeolite and the alumina is limited because the roughness of the alumina surface is smaller than the zeolite particle size.

Fig. 11 presents toluene ignition curves for the monoliths loaded with Pt/ZSM5 and that of the anodised foam monolith directly impregnated with Pt. Three main observations can be pointed. Firstly, the activity depends on the amount of Pt/ZSM5 loaded on the monolith. Secondly, Pt on zeolite is much more active than Pt directly supported on the anodised alumina, even the total amount of Pt is much higher on the monolith without zeolite. And finally, the foam monoliths present higher activity than longitudinal parallel channel monolith with similar amount of Pt/ZSM5 loaded.

4. Discussion

Previous studies carried out in our laboratory using aluminium sheets [12] showed that texture of the anodisation alumina is the result of two concurrent processes, i.e., the alumina generation and its dissolution inside the pores. These pores are perpendicular to the surface and this enables the electrical current to be transported by the electrolyte that fills these pores, while dissolved ions are transported out of the

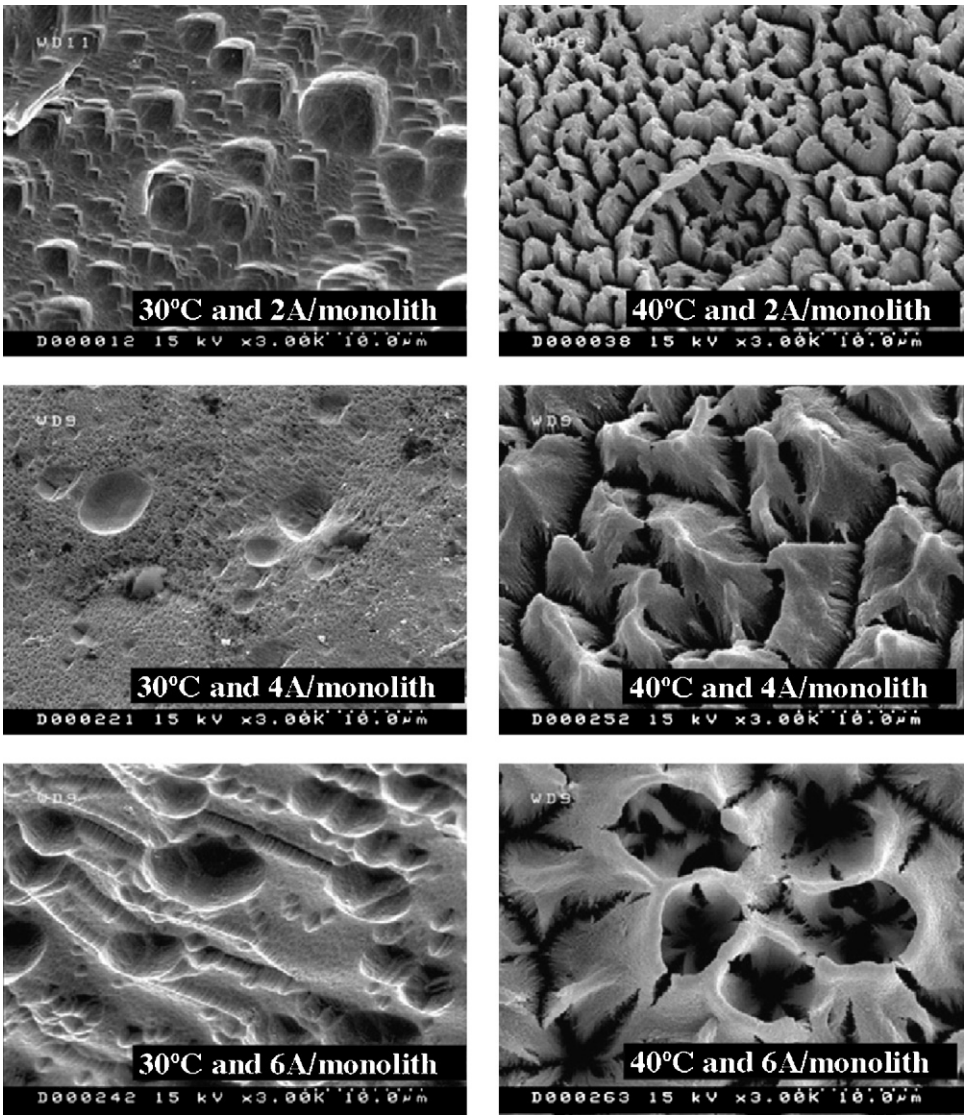

Fig. 5. SEM micrographs. Effect of anodisation current density on alumina layer (2.55 M H_2SO_4, 30–40 °C and 20 min).

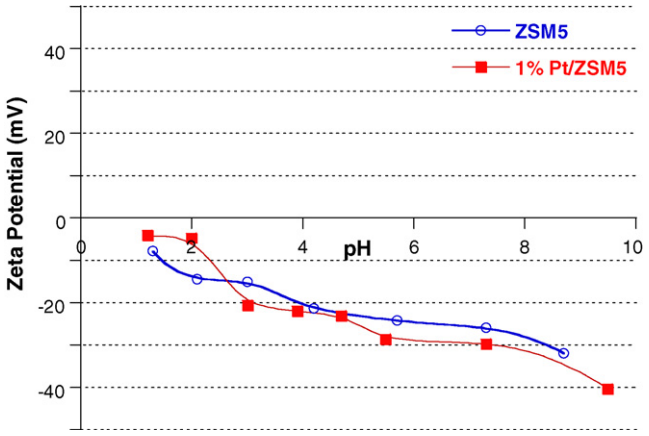

Fig. 6. Zeta Potential dependence on pH for NH_4-ZSM5 zeolite and 1% Pt-ZSM5 catalyst.

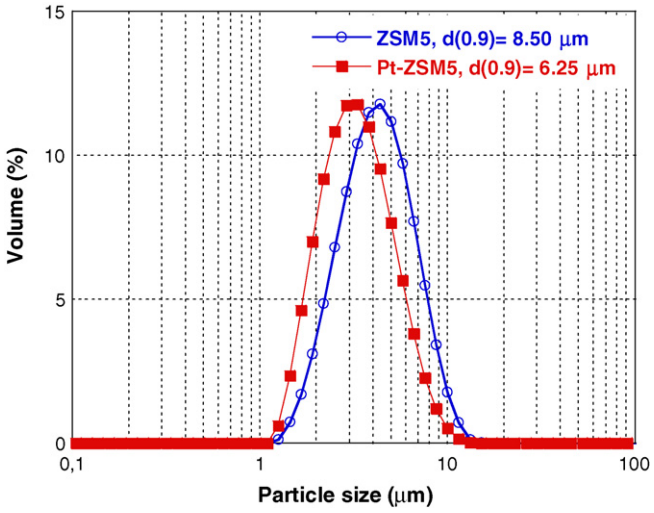

Fig. 7. Particle size distributions for the NH_4-ZSM5 zeolite and 1% Pt-ZSM5 catalyst.

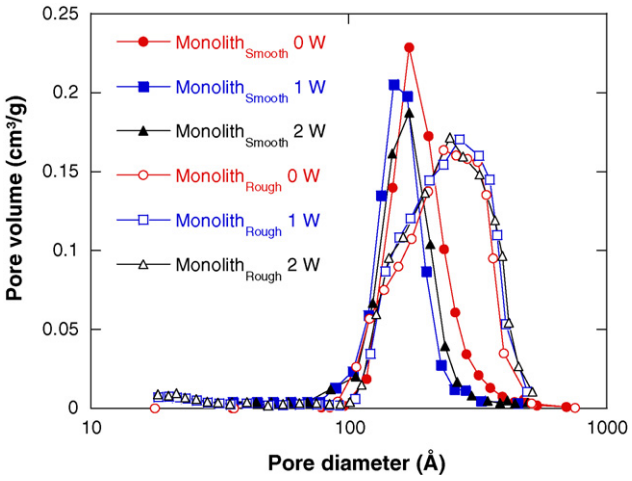

Fig. 8. Pore size distribution.

anodisation layer. Pores are not perfectly cylindrical, showing an increase in diameter from the bottom to the mouth. The main conclusions of the previous study on sheets are also relevant in the case of the aluminium foams used in this work.

Among the anodisation variables, temperature is one of the most important. In the series carried out with 2 A/monolith for 20 min from 10 to 60 °C, it can be shown that until 30 °C the amount of alumina generated is more or less the same (g of alumina per monolith and thickness) but the pore volume and surface area increase although pores have the same size. This fact suggests that the increase in surface area and porosity must be produced by an increase in the number of pores. At 40 °C the amount of alumina produced and retained by the anodised monoliths decreases significantly although the surface area and porosity of the monolith increase showing a dramatic increase in the surface area, porosity and pore size of the alumina. This

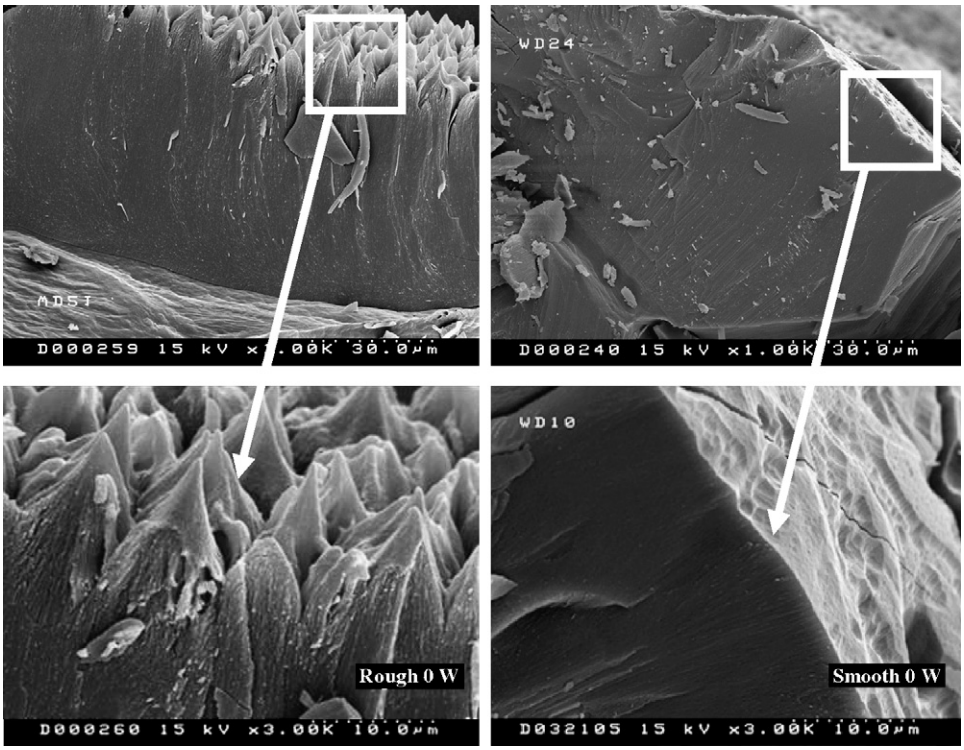

Fig. 9. SEM micrographs of alumina layer.

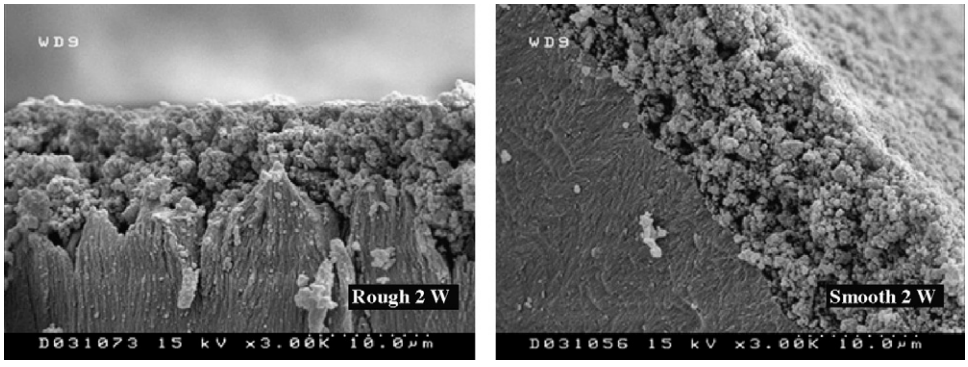

Fig. 10. SEM micorgraphs of alumina layer coated with Pt-ZSM5.

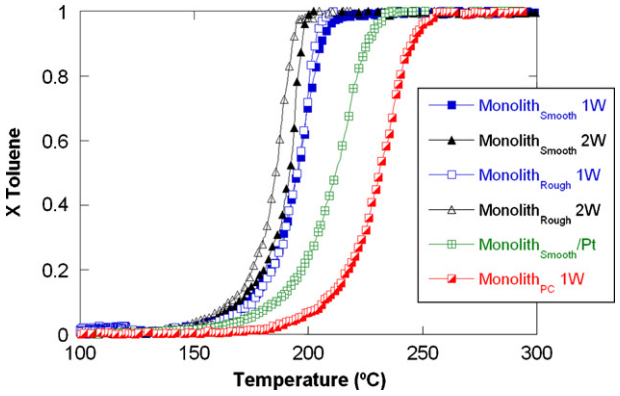

Fig. 11. Toluene ignition curves.

must be due to an increase in the alumina dissolution process that also produces a qualitative change in the outer side of the alumina layer (see Figs. 3 and 9). The external surface of the alumina cannot continue the coherent growing (Fig. 9 right) and deep cracks appear all over the surface (Fig. 3). The increase in temperature up to 50 and 60 °C favours so much the dissolution of alumina that the amount retained by the foam decreases drastically and the total surface area and porosity also decrease despite the increase of the specific textural properties of the remaining alumina. The cracking phenomenon is general on the surface. However, the size of the cracks decreases significantly when increasing temperature.

The cracking phenomenon also depends on anodisation time. In the series anodised at 30 °C and 2 A/monolith, during the 20 first minutes no cracking was detected (Fig. 4). On the other hand, at 40 min the thickness of the layer has continued growing with respect to the 20 min sample. However, the amount of alumina is lower because the porosity has increased dramatically and consequently, the surface area also increases. This change is accompanied by a significant cracking of the surface (Fig. 4). In the experiments carried out at 30 °C for 20 min of anodisation, the current density was increased from 2 to 6 A per monolith. This produced an increase in the amount of alumina layer and the corresponding increase in the textural properties, but it did not produce cracking (Fig. 5). The same series at 40 °C shows a similar increase in the amount of alumina and in textural properties. However, cracking is present in those three samples (Fig. 5) and cracks increase in size with increasing current density. The cracking phenomenon also produces wider pores as it can be seen comparing pore size distributions presented in Fig. 8.

The singular morphology of the cracked alumina surface offers interesting opportunities to fix catalytic coatings on aluminium foams to prepare structured catalytic systems. Indeed, as discussed in the introduction, anchoring and interlocking of the washcoat particles with the surface irregularities of the support play an important role on the adhesion of a washcoat to the support [15]. In this way, in order to enhance this mechanical adhesion, the size of the washcoat particles must be smaller than the size of the support macropores [18]. Therefore, an anodisation treatment of the alumina foam under conditions that produce surface cracks that are wider than the zeolite particle size should increase the adhesion of catalyst washcoating.

Another important phenomenon during ceramic monolith washcoating is the absorption of part of the slurry solvent by the ceramic porosity that concentrate part of the slurry solid, similar to the cake formation phenomenon during filtration [22].

In order to check these hypotheses, a comparison was performed using monolith anodised under two different conditions to obtain similar alumina coatings in thickness, surface area and porosity, but showing a conventional smooth surface or a deeply cracked one. Additionally, a non-anodised monolith was also used to check the eventual role of the alumina porosity (filtration cake effect). The amount of solid retained after the first washcoating (see Table 3) shows no filter cake effect by comparing the non-anodised monolith (0.0116 g) and the smooth one (0.0106 g). However, a clear increase in the case of the cracked surface (0.0179 g) is observed. After the second washcoating, the smooth monolith showed the highest increase (0.0178 g), a slightly lower increase the rough one (0.0149 g) and only 0.0099 g the non-anodised one.

The weight loss after the ultrasound test offers relevant information. The adhesion is much more firm in the case of the cracked monolith, showing 40–48% weight loss after the adhesion test instead of 80–85% in the case of the smooth monolith. This difference can be related to mechanical anchoring caused by the presence of deep cracks that allocate the zeolite particles (Fig. 10). Weight loss percentage after the first and the second washcoating is similar. Therefore, it can be concluded that the cohesion between the zeolite particles is similar to the adhesion between the zeolite coating and the anodised aluminium foam. In other words, the stability of the coating is controlled by both the interface between the zeolite and the foam, and the cohesion of the zeolite film. Finally, the dramatic weight loss of the non-anodised monolith indicates that the chemical compatibility or the texture of the alumina layer play also certain role in the coating adhesion.

Finally, and obviously the most important in the preparation of a catalytic device, the activity of the coated monoliths for total toluene oxidation is very high reaching complete conversion below 200 °C. The catalytic activity results obtained indicate the importance of the load of the active phase (platinum): the activity increases with increasing Pt load. This result agrees with those obtained by Burgos et al. [23], who observed that a higher amount of platinum or palladium, improved the activity of monoliths of longitudinal channel in the total oxidation of toluene. The higher activity of Pt on zeolite than on alumina could be related to a higher toluene adsorption capacity of the zeolite [24] or to the role of the acidity of the Pt support reported by different authors [25,26].

The foam monoliths present higher activity in the total oxidation of toluene than longitudinal parallel channel monoliths. Giani et al. [27] attributed this improvement to higher heat and mass transfer. Monoliths with longitudinal parallel channels usually develop laminar flows, whereas foams improve the mass transfer to the wall, as well as the radial temperature and composition homogeneity, mixing the flow between channels, which would lead to an improvement in the turbulence [3–5].

5. Conclusions

Aluminium foams can be anodised under different conditions to produce alumina coatings with controlled textural properties. When anodisation conditions are extreme, an important cracking of the surface appears with width and depth cracks that depend on the anodisation parameters. The roughness of the surface can be used to improve the adhesion of Pt/ZSM5 coatings because the size of the cracks is wide enough to occlude the zeolite particles, promoting a mechanical anchorage of the coating. In this way, very active catalytic devices have been prepared and tested in total oxidation of toluene.

Acknowledgements

Financial support by UPV/EHU (9/UPV0021.215-14499/2002) and MEC (ref. MAT2003-06540-C02) are gratefully acknowledged.

References

[1] F.-C. Buciuman, B. Kraushaar-Czarnetzki, Catal. Today 69 (2001) 337–342.
[2] ERG: www.ergaerospace.com/duocel_foam.
[3] L. Giani, G. Groppi, E. Tronconi, Ind. Eng. Chem. Res. 44 (24) (2005) 9078–9085.
[4] O.Y. Podyacheva, A.A. Ketov, Z.R. Ismagilov, V.A. Ushakov, A. Bos, H.J. Veringa, React. Kinet. Catal. Lett. 60 (1997) 243–250.
[5] J.T. Richardson, M. Garrait, J.-K. Hung, Appl. Catal. A 255 (1) (2003) 69–82.
[6] T.A. Nijhuis, A.E.W. Beers, T. Vergunst, I. Hoek, F. Kapteijn, J.A. Moulijn, Catal. Rev. 43 (4) (2001) 345–380.
[7] T.H. Elmer, US Patent 3,958,058 (1976).
[8] D.A. Hickman, L.D. Schmidt, J. Catal. 136 (2) (1992) 300–308.
[9] M.F.M. Zwinkels, S.G. Järas, P.G. Menon, K.J. Aasen, J. Mater. Sci. 31 (1996) 6345–6349.
[10] N. Burgos, M. Paulis, A. Gil, L.M. Gandia, M. Montes, Stud. Surf. Sci. Catal. 130A (2000) 593–598.
[11] L. Wang, M. Sakurai, H. Kameyama, J. Chem. Eng. Jpn. 37 (2) (2004) 1513–1520.
[12] N. Burgos, M. Paulis, M. Montes, J. Mater. Chem. 13 (6) (2003) 1458–1467.
[13] P. Avila, M. Montes, E.E. Miró, Chem. Eng. J. 109 (2005) 11–36.
[14] C. Agrafiotis, A. Tsetsekou, A. Ekonomakau, J. Mater. Sci. Lett. 18 (1999) 1421–1424.
[15] C. Agrafiotis, A. Tsetsekou, J. Eur. Ceram. Soc. 20 (2000) 815–824.
[16] C. Agrafiotis, A. Tsetsekou, J. Eur. Ceram. Soc. 20 (2000) 825–834.
[17] J.M. Zamaro, M.A. Ulla, E.E. Miró, Chem. Eng. J. 106 (2005) 25–33.
[18] P. Cini, S.R. Blaha, M.P. Harold, J. Membr. Sci. 55 (1991) 199–225.
[19] S. Yasaki, Y. Yoshino, K. Ihara, K. Ohkubo, US Patent 5,208,206 (1993).
[20] L. Lizarbe Ruiz, in ‘‘Teoría y Práctica de la Lucha Contra la Corrosión’’, J.A. González Fernández (Ed.), Grafimad S.A., Madrid, 1984.
[21] F. Scheffler, R. Herrmann, W. Schwieger, M. Scheffler, Microporous Mesoporous Mater. 67 (2004) 53–59.
[22] W.B. Kolb, A.A. Papadimitriou, R.L. Cerro, D.D. Leavitt, J.C. Summers, Chem. Eng. Prog. 89 (1993) 61–67.
[23] N. Burgos, M. Paulis, J. Sambeth, J.A. Odriozola, M. Montes, Studies Surf. Sci. Catal. 118 (1998) 157–166.
[24] T.F. Garetto, E. Rincón, C.R. Apesteguía, Appl. Catal. B: Environ. 48 (2004) 167–174.
[25] Y. Yazawa, N. Kagi, S. Komai, A. Satsuma, Y. Murakami, T. Hattori, Catal. Lett. 72 (2001) 157–160.
[26] Y. Yazawa, H. Yoshida, T. Hattori, Appl. Catal. A: Gen. 237 (2002) 139–148.
[27] L. Giani, G. Groppi, E. Tronconi, Ind. Eng. Chem. Res. 44 (2005) 4993–5002.